Mathematical Biosciences 326 (2020) 108395

Contents lists available at ScienceDirect

Mathematical Biosciences

journal homepage: www.elsevier.com/locate/mbs

Original Research Article

Effects of periodic intake of drugs of abuse (morphine) on HIV dynamics: Mathematical model and analysis

Jones M. Mutua [a], Feng-Bin Wang [b,c], Naveen K. Vaidya [d,e,f,*]

[a] Department of Computer Science, Mathematics, & Physics, Missouri Western State University, St. Joseph, MO, USA
[b] Department of Natural Science in the Center for General Education, Chang Gung University, Guishan, Taoyuan 333, Taiwan
[c] Community Medicine Research Center, Chang Gung Memorial Hospital, Keelung Branch, Keelung 204, Taiwan
[d] Department of Mathematics and Statistics, San Diego State University, San Diego, CA, USA
[e] Computational Science Research Center, San Diego State University, San Diego, CA, USA
[f] Viral Information Institute, San Diego State University, San Diego, CA, USA

ARTICLE INFO

Keywords:
Drugs of abuse
Global stability
Infection threshold
Morphine pharmacodynamics
Non-autonomous system

ABSTRACT

Drugs of abuse, such as opiates, have been widely associated with diminishing host-immune responses, including suppression of HIV-specific antibody responses. In particular, periodic intake of the drugs of abuse can result in time-varying periodic antibody level within HIV-infected individuals, consequently altering the HIV dynamics. In this study, we develop a mathematical model to analyze the effects of periodic intake of morphine, a widely used opiate. We consider two routes of morphine intake, namely, intravenous morphine (IVM) and slow-release oral morphine (SROM), and integrate several morphine pharmacodynamic parameters into HIV dynamics model. Using our non-autonomous model system we formulate the infection threshold, $\mathcal{R}_i$, for global stability of infection-free equilibrium, which provides a condition for avoiding viral infection in a host. We demonstrate that the infection threshold highly depends on the morphine pharmacodynamic parameters. Such information can be useful in the design of antibody-based vaccines. In addition, we also thoroughly evaluate how alteration of the antibody level due to periodic intake of morphine can affect the viral load and the CD4 count in HIV infected drug abusers.

1. Introduction

Human Immunodeficiency Virus (HIV), the infectious agent for the global AIDS epidemic, remains one of the major public health challenges. Over 33 million people worldwide currently live with the virus, while 1.8 million new infections and 1 million AIDS-related deaths are estimated to occur annually [1,2]. Among the people living with HIV, the frequency of use and dependence on drugs of abuse, such as opiates, is rapidly increasing [3,4]. As a result, drug abusers constitute a large cohort within the HIV-infected population [3,4]. For example, as estimated by the Center for Disease Control and Prevention [5], in the US about one third of the total AIDS cases and the annual new HIV cases were linked to the use of drugs of abuse. These statistics show that there exists a significant public health burden due to the use of drugs of abuse among HIV infected populations. Thus detailed studies on HIV infection in drug abusers are in high demand to help design HIV control strategies suitable for drug abusers.

It is known that HIV-infected drug abusers are at a greater risk of suffering from higher viral load, rapid disease progression, and diminished host-immune responses [6–10]. Importantly, presence of drugs of abuse, such as morphine, can significantly reduce the HIV-specific antibody levels in a host [7,8]. Since these antibodies are known to play a role in controlling established HIV infection and preventing new infections [11], it is critical to understand how drugs of abuse affect the viral dynamics within HIV-infected individuals. Analysis of morphine-altered antibody responses impacting viral dynamics is particularly important for devising antibody mediated controls for drug abusers.

Mathematical modeling has been useful in understanding the dynamics of systems with virus infections and immune responses [12–17]. However, limited study has been done relating to modeling of HIV dynamics under conditioning of drugs of abuse [13,17]. In particular, using experimental data from simian immunodeficiency virus infection of morphine-addicted macaques [7,8], we previously developed a mathematical model to quantify effects of morphine on antibody responses and virus dynamics [13]. While these studies [13,17] have offered important results on relations among morphine conditioning, antibody responses and viral dynamics, they have utilized constant morphine conditioning that primarily represents experimental setting [7,8], in which constant morphine within animal body is maintained. However, in many cases, drugs of abuse are often taken periodically, including

* Corresponding author. *Mailing address*: 5500 Campanile Drive, San Diego, CA 92182 USA.
E-mail address: nvaidya@sdsu.edu (N.K. Vaidya).

https://doi.org/10.1016/j.mbs.2020.108395
Received 12 December 2019; Received in revised form 27 May 2020; Accepted 27 May 2020
Available online 30 May 2020

slow-release oral morphine (SROM) that is given to drug abusers for treatment and/or during rehabilitation. In such periodic intake, the concentration of drugs of abuse changes periodically over time resulting in periodic changes of virus-specific antibody concentrations within a host. Therefore, to accurately evaluate the effects of morphine conditioning on antibody responses and virus dynamics, it is important to consider time-varying morphine concentration, including the case in which morphine is taken periodically.

In this study, we develop and analyze a model describing within-host HIV dynamics under periodic morphine intake. We consider two routes of morphine intake, namely, intravenous morphine (IVM) and slow-release oral morphine (SROM), and integrate several morphine pharmacodynamic parameters into HIV dynamics model. We thoroughly perform mathematical analysis of our non-autonomous model system, and establish the local as well as global properties of the viral dynamical system, including the formulation of infection threshold, $\mathcal{R}_i$. Furthermore, we evaluate how pharmacodynamics of morphine affect the various aspects of viral dynamics in HIV-infected drug abusers. As revealed by our results, the novel feature in our model, namely, a more realistic time-dependent morphine implying time-dependent antibody changes, can have significant impact on the viral dynamics as well as on the determinants of infection persistence. These results can provide new insights into the virus control through immune responses under conditioning of drugs of abuse. Furthermore, the time-dependent antibody changes provide a non-autonomous model, which requires sophisticated mathematical techniques for its analysis. In particular, the infection-free equilibrium of our model is determined by a two-dimensional system, instead of commonly available viral dynamics model with one dimensional infection-free equilibrium, and our full model is a time-periodic system, which enhance further mathematical challenges. By using theory of monotone dynamical system, the comparison principle and theory of uniform persistence, we are able to establish a threshold result on the global dynamics of the proposed HIV model in terms of infection threshold, $\mathcal{R}_i$. Fairly rigorous analysis presented in this paper can also be applied to other non-autonomous systems, for which analytical techniques have not been widely advanced in comparison to autonomous systems.

2. Model development

2.1. Modeling virus dynamics with effects of HIV-specific antibodies

We assume that target cells of HIV ($CD4^+$ T cells) are generated at a constant rate λ and die at per capita rate d. Based on the previously established models [13,17], we divide target cells into two subpopulations: T_l (with lower susceptibility to infection due to low level of co-receptor expression) and T_h (with higher susceptibility to infection due to high level of co-receptor expression). These subpopulations switch from T_l to T_h and T_h to T_l with the transition rates r and q, respectively. Upon interaction with free virus (V), target cells, T_l and T_h, become infected (I) at rates β_l and β_h, respectively. δ and c represent a per capita death rate of infected cells and a per capita clearance rate of virions. Infected cells produce virus at a rate p per infected cell.

In our previous study [13], we established that the model with two major effects of HIV-specific antibodies, namely reduction of virus-specific infectivity and enhancement of virus clearance, best describes experimental data. Following this result, we incorporate time-varying efficacy, $\Omega_I(t)$, of virus-specific antibodies in the reduction of virus infectivity and time-varying enhancement, $\Omega_c(t)$, of virus clearance due to antibody binding to cell-free virus, into the viral dynamics model. Consequently, the HIV specific-antibodies result in the following three substitutions in our model: $\beta_l \to [1-\Omega_I(t)]\beta_l$, $\beta_h \to [1-\Omega_I(t)]\beta_h$, and $c \to [c+\Omega_c(t)]$. Note that we did not consider possible effects of antibodies on suppressing infected cells because the model with this effect was not supported by the experimental data from macaques under morphine conditioning [13]. Even though this effect is not incorporated here, our model can easily be extended to include the possible suppression of infected cells by antibodies as done in previous studies [13,18] and our analytical techniques can be applied to the extended model.

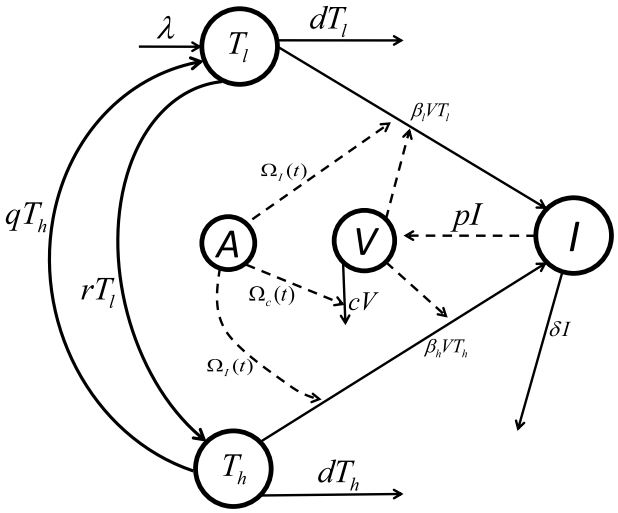

Fig. 1. Schematic diagram of the virus and antibody dynamics model.

Following the previous models [13,19] supported by the experimental data, here we consider the antibody dynamics via an explicit function, which is assumed to take into account all factors, including effects from virus particles. In this approach, influence of virus on antibody response is indirectly captured through parameters in the explicit form of antibody concentration profile. As done previously [13,19], we define $\Omega_I(t)$ and $\Omega_c(t)$ as $\Omega_I(t) = \frac{\eta A(t)}{1+\eta A(t)}$ and $\Omega_c(t) = \sigma A(t)$, where $A(t)$ represents the time-varying HIV-specific antibody responses. Moreover, following the traditional drug-response mechanism, we model the dependency of HIV-specific antibody responses on the morphine concentration using the formula $A(t) = \left(1 - \frac{M(t)^n}{M_h^n + M(t)^n}\right)$, where $M(t)$ represents morphine concentration at time t, M_h represents the morphine concentration when antibody response is half of the maximum response, and n is the Hill coefficient. $A(t)$ is formulated in such a way that its value lies between 0 and 1 with $A(t) = 0$ for a very high morphine concentration (i.e., $M(t) \to \infty$) and $A(t) = 1$ (maximum) in the absence of morphine (i.e., $M(t) = 0$), consistent with the previous experimental and theoretical results on the effect of morphine on antibody responses [8,13]. An example of a graph describing the dependence of antibody responses, $A(t)$, on the morphine concentration is shown in Fig. 2(a). We describe the virus and antibody dynamics using the following set of equations:

$$\begin{cases} \frac{dT_l}{dt} = \lambda + qT_h - dT_l - rT_l - [1-\Omega_I(t)]\beta_l V T_l, \\ \frac{dT_h}{dt} = rT_l - dT_h - qT_h - [1-\Omega_I(t)]\beta_h V T_h, \\ \frac{dI}{dt} = [1-\Omega_I(t)]\beta_l V T_l + [1-\Omega_I(t)]\beta_h V T_h - \delta I, \\ \frac{dV}{dt} = pI - cV - \Omega_c(t)V, \\ T_l(0) = T_{l0},\ T_h(0) = T_{h0},\ I(0) = I_0,\ V(0) = V_0, \end{cases} \tag{1}$$

where

$$\Omega_I(t) = \frac{\eta A(t)}{1+\eta A(t)}, \quad \Omega_c(t) = \sigma A(t), \quad A(t) = 1 - \frac{M(t)^n}{M_h^n + M(t)^n}.$$

The schematic diagram of the model is presented in Fig. 1.

2.2. Modeling periodic morphine intake and pharmacodynamics

Since morphine, or drug of abuse in general, is often taken periodically, in our model we assume that the morphine concentration, $M(t)$,

is periodic function of period τ, i.e., $M(t) = M(t+\tau)$. As a consequence, time-varying parameters $\Omega_I(t)$ and $\Omega_c(t)$ become periodic functions of period τ, i.e., $\Omega_I(t) = \Omega_I(t+\tau)$ and $\Omega_c(t) = \Omega_c(t+\tau)$, respectively. We consider two common routes of morphine intake: intravenous morphine (IVM) and slow release oral morphine (SROM). The models for pharmacodynamics of morphine, time-varying morphine profile, and periodic intake via these two routes are describes below.

Intravenous morphine (IVM). In this case, morphine is directly injected into the blood stream. One reason why IVM may be preferred by drug abusers is that its direct administration into the circulation provides a rapid effect [20]. A previous study on pharmacokinetics and pharmacodynamics of opioids [21] has shown that the concentration profile of drugs administered via intravenous route is best described by an exponential decay function. Thus, we consider a function of the form $M(t) = a_0 e^{-b_1 t}$ to explain the dynamics of intravenous morphine concentration for a period of single intake. Therefore, for a periodic intake of IVM we model the morphine concentration as

$$M(t) = a_0 e^{-b_1(t-t_k)}, \qquad t_k \le t < t_{k+1}, \quad k = 0, 1, 2, \ldots \tag{2}$$

where, the period $\tau = t_{k+1} - t_k$ represents the time interval between two consecutive morphine intakes, a_0 represents the morphine dose, and b_1 denotes the decay rate. Note that $t_{1/2} = \ln(2)/b_1$ gives the half-life of morphine. Since the half-life of morphine is short as measured in the experiment [22], we ignored potential residual morphine from the previous period so that each interval begins with the initial morphine concentration of a_0. To support our assumption, we also computed the morphine concentration using residual morphine effect and found almost no difference on the net concentration. A graph describing the periodic morphine profile, $M(t)$, in the case of IVM is shown in Fig. 2(b).

Slow-release oral morphine (SROM). In this case, morphine is taken orally. SROM can be used as a maintenance pharmacotherapy treatment for opioid-dependent individuals who respond poorly to other available maintenance treatments [23]. It has also been reported that SROM may be associated with reduced opioid craving [24–30]. Moreover, the use of SROM among HIV-infected persons may present an additional safety advantage due to its lower risk with interactions with other drugs [31]. In using the SROM as a maintenance treatment, it is critical to identify the right balance between the need for the drug and its addictiveness. In oral morphine intake [32], the concentration of morphine in the blood slowly increases and then decreases after it reaches a peak. As supported by the experimental data [32], this phenomenon can approximately be captured using a function of the form

$$M(t) = M_0 + a\sin(\frac{2\pi}{\tau}t + b), \tag{3}$$

where M_0 represents the mean level of morphine, a denotes the amplitude, and b represents the phase shift in the function. A graph describing the periodic morphine profile, $M(t)$, in the case of SROM is shown in Fig. 2(c).

3. Mathematical analysis

In the rest of this paper, we shall consider the model system (1), where $\Omega_I(t)$ and $\Omega_c(t)$ are τ-periodic functions. We first show that $\mathbb{R}^4_+$ is positively invariant for (1). For any $(T_{l0}, T_{h0}, I_0, V_0) \in \mathbb{R}^4_+$, it follows from Theorem 5.2.1 in [33] that system (1) admits a unique local nonnegative solution $(T_l(t), T_h(t), I(t), V(t)) \in \mathbb{R}^4_+$ through the initial value $(T_l(0), T_h(0), I(0), V(0)) = (T_{l0}, T_{h0}, I_0, V_0)$. Let the total cell population be $N(t)$, i.e.,

$$N(t) = T_l(t) + T_h(t) + I(t). \tag{4}$$

Then it follows from the first three equations of (1) that

$$\frac{dN(t)}{dt} = \lambda - dT_l - dT_h - \delta I \le \lambda - d_{\min} N(t), \tag{5}$$

where $d_{\min} = \min\{d, \delta\}$. Here, we can take $d_{\min} = d$ as the life-span of infected cell ($\sim$ 1 day) is extremely shorter than the life-span of uninfected cell ($\sim$ 100 days), i.e., $d \ll \delta$. By the comparison principle, we see that $\limsup_{t\to\infty} N(t) \le \frac{\lambda}{d}$, that is, $N(t)$ is ultimately bounded. By the positivity of solutions of (1), it follows that $T_l(t)$, $T_h(t)$, and $I(t)$ are ultimately bounded. Then there exist a $t_0 > 0$ and $\chi > 0$ such that $I(t) \le \chi$, $\forall\ t \ge t_0$. In view of the fourth equation of (1), we see that

$$\frac{dV}{dt} \le p\chi - cV, \ \forall\ t \ge t_0.$$

The above inequality and the comparison principle imply that $\limsup_{t\to\infty} V(t) \le \frac{p\chi}{c}$, that is, $V(t)$ is ultimately bounded.

From the above discussion and Theorem 3.4.8 in [34], we have the following result:

Lemma 1. *$\mathbb{R}^4_+$ is positively invariant for system (1) and the system (1) admits a unique and bounded solution with the initial value in $\mathbb{R}^4_+$. Further, the system (1) admits a connected global attractor on $\mathbb{R}^4_+$ which attracts all positive orbits in $\mathbb{R}^4_+$.*

3.1. Infection threshold ($\mathcal{R}_i$)

In this section we use our periodic model system (1) to formulate an infection threshold, $\mathcal{R}_i$, which provides a condition for an infection to die out or persist. Bacaër and Guernaoui [35] proposed a general definition of such threshold for a vector-borne disease model with seasonality in periodic habitats. Similarly, Wang and Zhao [36] further introduced a computational formula for periodic compartmental epidemic models and showed that it is a threshold parameter for the local stability of the disease-free periodic solution. Here, we use a similar approach developed by Wang and Zhao [36] and introduce the infection threshold, $\mathcal{R}_i$, for periodic morphine intake system (1) of virus and antibody dynamics.

We first determine the infection-free equilibrium, E_0. To this end, we put $I = V = 0$ in system (1) and we arrive at the following system

$$\begin{cases} \frac{dT_l}{dt} = \lambda + qT_h - (d+r)T_l, \\ \frac{dT_h}{dt} = rT_l - (d+q)T_h, \\ T_l(0) = T_{l0},\ T_h(0) = T_{h0}. \end{cases} \tag{6}$$

It is easy to obtain that

$$(T_l^*, T_h^*) = \left(\frac{\lambda(d+q)}{d(d+q+r)}, \frac{\lambda r}{d(d+q+r)}\right) \tag{7}$$

is the unique positive equilibrium of system (6). Since system (6) is cooperative (see, e.g., [33]) and it admits a unique positive equilibrium (T_l^*, T_h^*), we obtain the following result related to the global stability of (T_l^*, T_h^*) (see, e.g., [37]).

Lemma 2. *System (6) admits a unique positive equilibrium (T_l^*, T_h^*) which is globally attractive in $\mathbb{R}^2_+$, that is, for any $(T_l(0), T_h(0)) \in \mathbb{R}^2_+$, we have*

$$\lim_{t\to\infty}(T_l(t), T_h(t)) = (T_l^*, T_h^*).$$

In view of Lemma 2, the infection-free equilibrium, E_0, takes the following form

$$E_0 = \left(\frac{\lambda(d+q)}{d(d+q+r)}, \frac{\lambda r}{d(d+q+r)}, 0, 0\right).$$

The equations for the infected cells and virus compartments of the linearized system at the infection-free equilibrium, E_0, take the form

$$\begin{cases} \frac{dI}{dt} = -\delta I + \frac{\lambda[1-\Omega_I(t)]}{d(d+q+r)}[\beta_l(d+q) + \beta_h r]V, \\ \frac{dV}{dt} = pI - [c + \Omega_c(t)]V. \end{cases} \tag{8}$$

We now introduce two matrices

$$\mathcal{F}(t) = \begin{pmatrix} 0 & \frac{\lambda[1-\Omega_I(t)]}{d(d+q+r)}[\beta_l(d+q) + \beta_h r] \\ 0 & 0 \end{pmatrix},$$

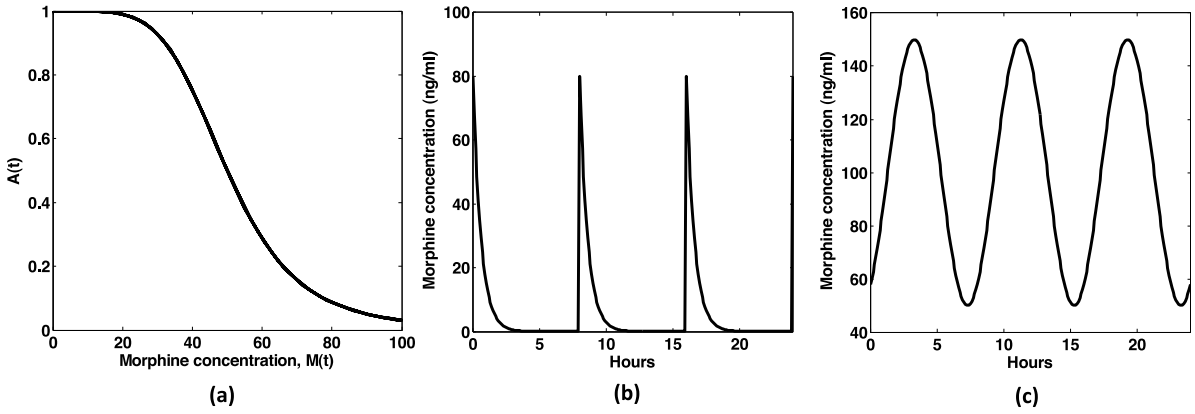

Fig. 2. (a) HIV-specific antibody response, $A(t)$, as a function of morphine concentration, $M(t)$; (b) Periodic morphine concentration profile, $M(t)$, in the case of IVM; and (c) Periodic morphine concentration profile, $M(t)$, in the case of SROM.

$$\mathcal{V}(t) = \begin{pmatrix} \delta & 0 \\ -p & c+\Omega_c(t) \end{pmatrix}.$$

For a given τ-periodic function $\mathbb{V}(t)$, we will use $\Phi_{\mathbb{V}(\cdot)}(t)$ to represent the monodromy matrix of the linear τ-periodic differential system $\frac{dz(t)}{dt} = \mathbb{V}(t)z$, and we use $\rho(\Phi_{\mathbb{V}(\cdot)}(\tau))$ to denote the spectral radius of $\Phi_{\mathbb{V}(\cdot)}(\tau)$.

We now assume that $Y(t,s)$, $t \geq s$ is the evolution operator of the linear τ-periodic system

$$\frac{dy}{dt} = -\mathcal{V}(t)y. \tag{9}$$

That is, for each $s \in \mathbb{R}$, the 2×2 matrix $Y(t,s)$ satisfies

$$\frac{d}{dt}Y(t,s) = -\mathcal{V}(t)Y(t,s) \quad \forall t \geq s, \quad Y(s,s) = I,$$

where I is the 2×2 identity matrix. Then the monodromy matrix of (9), $\Phi_{-\mathcal{V}}(t)$, equals $Y(t,0)$, $t \geq 0$.

Let $\phi(s)$, τ-periodic in s, be the initial distribution of virus particles. Then $\mathcal{F}(s)\phi(s)$ is the rate of new infected cells produced by the virus particles which were introduced at time s. Given $t \geq s$, then $Y(t,s)\mathcal{F}(s)\phi(s)$ provides the distribution of those virus particles which were newly produced by infected cells at time s and remain in the virus compartment at time t.

Let C_τ be the ordered Banach space of τ-periodic functions from $\mathbb{R}$ to $\mathbb{R}^2$ with the maximum norm $\|.\|$ and the positive cone $C_\tau^+ := \{\phi \in C_\tau : \phi(t) \geq 0 \ \ \forall t \in \mathbb{R}\}$. We now define a linear operator $\mathcal{L} : C_\tau \to C_\tau$ by

$$(\mathcal{L}\phi)(t) = \int_0^\infty Y(t, t-a)\mathcal{F}(t-a)\phi(t-a), \ \forall t \in \mathbb{R}, \phi \in C_\tau.$$

Here, $\int_0^\infty Y(t,t-a)\mathcal{F}(t-a)\phi(t-a)da = \int_{-\infty}^t Y(t,s)\mathcal{F}(s)\phi(s)ds$ gives the distribution of accumulated new viruses at time t produced due to all those viruses $\phi(s)$ at times before t. Therefore, $\mathcal{L}$ is the next infection operator [36,38], and we define infection threshold as $\mathcal{R}_i = \rho(\mathcal{L})$, the spectral radius of $\mathcal{L}$.

As in Wang and Zhao [36] and Liu, Zhao and Zhou [39], we let $\mathcal{W}(t,s,\theta)$, $t \geq s$, $s \in \mathbb{R}$ be the monodromy matrix of the linear τ-periodic system on $\mathbb{R}^2$

$$\frac{dw}{dt} = \left(-\mathcal{V}(t) + \frac{\mathcal{F}(t)}{\theta}\right)w, \quad t \in \mathbb{R}, \tag{10}$$

with parameter $\theta \in (0,\infty)$. By Theorem 2.1 of [36], we have the following results.

Lemma 3. *The following statements hold*

(i) *If $\rho(\mathcal{W}(\tau,0,\theta)) = 1$ has a positive solution θ_0, then θ_0, is an eigenvalue of operator $\mathcal{L}$, and hence $\mathcal{R}_i > 0$.*
(ii) *If $\mathcal{R}_i > 0$, then $\theta = \mathcal{R}_i$ is the unique solution of $\rho(\mathcal{W}(\tau,0,\theta)) = 1$.*
(iii) *$\mathcal{R}_i = 0$ if and only if $\rho(\mathcal{W}(\tau,0,\theta)) < 1$ for all $\theta > 0$.*

By Theorem 2.2 in [36], we further have the following result:

Lemma 4 (*see Theorem 2.2 in [36]*)**.** *The following statements hold.*

(i) *$\mathcal{R}_i = 1$ if and only if $\rho(\Phi_{\mathcal{F}(\cdot)-\mathcal{V}(\cdot)}(\tau)) = 1$;*
(ii) *$\mathcal{R}_i > 1$ if and only if $\rho(\Phi_{\mathcal{F}(\cdot)-\mathcal{V}(\cdot)}(\tau)) > 1$;*
(iii) *$\mathcal{R}_i < 1$ if and only if $\rho(\Phi_{\mathcal{F}(\cdot)-\mathcal{V}(\cdot)}(\tau)) < 1$.*

Thus, the disease-free steady state E_0 is locally asymptotically stable if $\mathcal{R}_i < 1$, and unstable if $\mathcal{R}_i > 1$.

Homogeneous (constant morphine) case. We now briefly mention that $\mathcal{R}_i$ formulated above can also recover the basic reproduction number, R_0, that we derived previously for the dynamics when constant morphine is maintained [13]. In the homogeneous (constant morphine) case, $\Omega_I(t) \equiv \Omega_I$ and $\Omega_c(t) \equiv \Omega_c$ are both constants. Then $\mathcal{F}(t) \equiv \mathcal{F}$ and $\mathcal{V}(t) \equiv \mathcal{V}$ become two constant matrices. Substituting constant matrices $\mathcal{F}$ and $\mathcal{V}$, we obtain (see also [36,40])

$$\mathcal{R}_i = \rho(\mathcal{L}) = \rho(\mathcal{F}\mathcal{V}^{-1}).$$

By computations, we can obtain that

$$\mathcal{F}\mathcal{V}^{-1} = \begin{pmatrix} \frac{p}{\delta(c+\Omega_c)}\mathcal{F}_{12} & \frac{1}{c+\Omega_c}\mathcal{F}_{12} \\ 0 & 0 \end{pmatrix},$$

where $\mathcal{F}_{12} = \frac{\lambda[1-\Omega_I]}{d(d+q+r)}[\beta_l(d+q) + \beta_h r]$. Then $\mathcal{R}_i$ can be expressed as the following explicit form

$$\mathcal{R}_i = \frac{p}{\delta(c+\Omega_c)}\mathcal{F}_{12}.$$

Here, $\mathcal{R}_i = R_0$, which is the basic reproduction number [13] that we derived using the second generation matrix method [40] for constant morphine case.

3.2. Infection threshold mediated virus dynamics

In this section, we show that whether the virus infection is avoided/eradicated or infection persists within a host can be determined by the sign of $\mathcal{R}_i - 1$.

Let $\mathbb{X} = \mathbb{R}^4_+$. Suppose $P : \mathbb{X} \to \mathbb{X}$ is the Poincaré map associated with system (1), that is,

$$P(x^0) = u(\tau, x^0), \ \forall \ x^0 := (T_{l0}, T_{h0}, I_0, V_0) \in \mathbb{X},$$

where $u(t,x^0)$ is the unique solution of system (1) with $u(0,x^0) = x^0$. Then we can obtain

$$P^n(x^0) = u(n\tau, x^0), \ \forall \ n \geq 0.$$

Let

$$\mathbb{X}_0 := \{(T_l, T_h, I, V) \in \mathbb{X} : I > 0 \text{ and } V > 0\},$$

and

$$\partial\mathbb{X}_0 := \mathbb{X}\backslash\mathbb{X}_0 = \{(T_l, T_h, I, V) \in \mathbb{X} : I = 0 \text{ or } V = 0\}.$$

Lemma 5. *Assume that $(T_l(t), T_h(t), I(t), V(t))$ is a solution of the system (1) with initial value $(T_{l0}, T_{h0}, I_0, V_0) \in \mathbb{X}_0$. Then*

$$(T_l(t), T_h(t), I(t), V(t)) \gg 0, \ \forall\ t > 0.$$

Proof. Given any initial value $(T_{l0}, T_{h0}, I_0, V_0) \in \mathbb{X}_0$. In view of the first equation of system (1), it follows that

$$T_l(t) = e^{-\int_0^t b(s_1)ds_1}\left[\int_0^t e^{\int_0^{s_2} b(s_1)ds_1} a(s_2)ds_2 + T_{l0}\right], \tag{11}$$

where

$$a(t) := \lambda + qT_h(t) \geq \lambda > 0, \tag{12}$$

and

$$b(t) := d + r + [1 - \Omega_I(t)]\beta_l V(t). \tag{13}$$

Thus, $T_l(t) > 0, \ \forall\ t > 0$. In view of the second equation of system (1), it follows that

$$T_h(t) = e^{-\int_0^t \hat{b}(s_1)ds_1}\left[\int_0^t e^{\int_0^{s_2} \hat{b}(s_1)ds_1} \hat{a}(s_2)ds_2 + T_{h0}\right], \tag{14}$$

where

$$\hat{a}(t) := rT_l(t) > 0, \tag{15}$$

and

$$\hat{b}(t) := d + q + [1 - \Omega_I(t)]\beta_h V(t). \tag{16}$$

Thus, $T_h(t) > 0, \ \forall\ t > 0$.

Treating Theorem 4.1.1 of [33] as generalized to nonautonomous systems, the irreducibility of the cooperative matrix

$$\begin{pmatrix} -\delta & [1 - \Omega_I(t)][\beta_l T_l(t) + \beta_h T_h(t)] \\ p & -c - \Omega_c(t) \end{pmatrix} \tag{17}$$

implies that

$$(I(t), V(t))^T \gg 0, \ \forall\ t > 0. \tag{18}$$

This completes the proof. □

Lemma 6. *Let $\mathcal{R}_i > 1$. Then there exists $\delta_0 > 0$ such that for any $(T_{l0}, T_{h0}, I_0, V_0) \in \mathbb{X}_0$ with*

$$\|(T_{l0}, T_{h0}, I_0, V_0) - E_0\| \leq \delta_0,$$

we have

$$\limsup_{n\to\infty} \|P^n(T_{l0}, T_{h0}, I_0, V_0) - E_0\| \geq \delta_0.$$

Proof. Assume that $\mathcal{R}_i > 1$. Then Lemma 4 implies that $\rho(\Phi_{F(\cdot)-\mathcal{V}(\cdot)}(\tau)) > 1$. Thus, we can choose $\xi_0 > 0$ small enough such that $\rho(\Phi_{G_{\xi_0}(\cdot)}(\tau)) > 1$, where

$$G_{\xi_0}(t) = \begin{pmatrix} -\delta & [1 - \Omega_I(t)]\left[\beta_l(T_l^* - \xi_0) + \beta_h(T_h^* - \xi_0)\right] \\ p & -[c + \Omega_c(t)] \end{pmatrix}.$$

By the continuity of the solutions with respect to the initial values, there exists a $\delta_0 > 0$ such that for all $(T_{l0}, T_{h0}, I_0, V_0) \in \mathbb{X}_0$ with

$$\|(T_{l0}, T_{h0}, I_0, V_0) - E_0\| \leq \delta_0,$$

there holds $\|u(t, (T_{l0}, T_{h0}, I_0, V_0)) - u(t, E_0)\| < \xi_0, \ \forall\ t \in [0, \tau]$.

We now prove the following claim.

$$\limsup_{n\to\infty} \|P^n(T_{l0}, T_{h0}, I_0, V_0) - E_0\| \geq \delta_0.$$

Assume, by contradiction, that the above claim does not hold. Then we have

$$\limsup_{n\to\infty} \|P^n(T_{l0}, T_{h0}, I_0, V_0) - E_0\| < \delta_0,$$

for some $(T_{l0}, T_{h0}, I_0, V_0) \in \mathbb{X}_0$. Without loss of generality, we assume that

$$\|P^n(T_{l0}, T_{h0}, I_0, V_0) - E_0\| < \delta_0, \ \forall\ n \geq 0.$$

It follows that

$$\|u(t, P^n(T_{l0}, T_{h0}, I_0, V_0)) - u(t, E_0)\| < \xi_0, \ \forall\ t \in [0, \tau], \ n \geq 0.$$

For any $t \geq 0$, let $t = m\tau + t'$, where $t' \in [0, \tau)$, and m is the largest integer less than or equal to $\frac{t}{\tau}$. Therefore, we have

$$\begin{aligned}&\|u(t, (T_{l0}, T_{h0}, I_0, V_0)) - u(t, E_0)\| \\ &= \|u(t', P^m(T_{l0}, T_{h0}, I_0, V_0)) - u(t', E_0)\| < \xi_0.\end{aligned} \tag{19}$$

Note that

$$(T_l(t), T_h(t), I(t), V(t)) = u(t, (T_{l0}, T_{h0}, I_0, V_0))$$

and $u(t, E_0) = E_0, \ \forall\ t \geq 0$. It then follows from (19) that for all $t \geq 0$, we have

$$T_l^* + \xi_0 > T_l(t) > T_l^* - \xi_0 > 0, \ T_h^* + \xi_0 > T_h(t) > T_h^* - \xi_0 > 0.$$

From the third and fourth equations in (1), it follows that

$$\begin{cases} \frac{dI}{dt} \geq -\delta I + [1 - \Omega_I(t)]\left[\beta_l(T_l^* - \xi_0) + \beta_h(T_h^* - \xi_0)\right]V, \ t > 0, \\ \frac{dV}{dt} = pI - [c + \Omega_c(t)]V, \ t > 0. \end{cases} \tag{20}$$

Since $(T_{l0}, T_{h0}, I_0, V_0) \in \mathbb{X}_0$, it follows from Lemma 5 that

$$(T_l(t), T_h(t), I(t), V(t)) \gg 0, \ \forall\ t > 0.$$

Thus, we may fix a $\check{\iota}_0 > 0$ such that $(I(\check{\iota}_0), V(\check{\iota}_0)) \gg 0$. Now, we consider the following auxiliary system

$$\begin{cases} \frac{dI}{dt} = -\delta I + [1 - \Omega_I(t)]\left[\beta_l(T_l^* - \xi_0) + \beta_h(T_h^* - \xi_0)\right]V, \ t > 0, \\ \frac{dV}{dt} = pI - [c + \Omega_c(t)]V, \ t > 0. \end{cases} \tag{21}$$

According to Lemma 2.1 in [41], there exists a positive, τ-periodic function $(\check{I}(t), \check{V}(t))^T$ such that $\check{m}e^{\check{\Theta}(t-\check{\iota}_0)}(\check{I}(t), \check{V}(t))^T$ is a solution of system (21), where $\check{\Theta} := \frac{1}{\tau}\ln(\rho(\Phi_{G_{\xi_0}(\cdot)}(\tau))) > 0$, due to the fact $\rho(\Phi_{G_{\xi_0}(\cdot)}(\tau)) > 1$. Here, we also take $\check{m}$ satisfying

$$(I(\check{\iota}_0), V(\check{\iota}_0)) \geq \check{m}(\check{I}(\check{\iota}_0), \check{V}(\check{\iota}_0))^T.$$

The standard comparison theorem (see, e.g., Theorem B.1 in [42]) implies that

$$(I(t), V(t)) \geq \check{m}e^{\check{\Theta}(t-\check{\iota}_0)}(\check{I}(t), \check{V}(t))^T, \ \forall\ t \geq \check{\iota}_0.$$

In particular, there exists n_1 such that

$$(I(n\tau), V(n\tau)) \geq \check{m}e^{\check{\Theta}(n\tau-\check{\iota}_0)}(\check{I}(n\tau), \check{V}(n\tau))^T, \ \forall\ n \geq n_1.$$

Since $\check{\Theta} > 0$, it follows that $I(n\tau) \to \infty$ and $V(n\tau) \to \infty$ as $n \to \infty$. This contradiction completes the proof. □

The following result establishes that $\mathcal{R}_i$ is a threshold index determining whether infection is avoided/eradicated or persists.

Theorem 1. *The following statements hold.*

(i) *If $\mathcal{R}_i < 1$, then the unique infection-free equilibrium, $E_0 = (T_l^*, T_h^*, 0, 0)$ is globally asymptotically stable for system (1) in the sense that*

$$\lim_{t\to\infty}(T_l(t), T_h(t), I(t), V(t)) = E_0;$$

(ii) *If* $\mathcal{R}_i > 1$, *there exists an* $\zeta > 0$ *such that for any solution* $(T_l(t), T_h(t), I(t), V(t))$ *with initial value* $(T_{l0}, T_{h0}, I_0, V_0) \in \mathbb{X}_0$ *satisfies*

$$\liminf_{t\to\infty} I(t) \geq \zeta, \ \liminf_{t\to\infty} V(t) \geq \zeta.$$

Further, system (1) admits at least one positive τ*-periodic solution*

$$(\hat{T}_l(t), \hat{T}_h(t), \hat{I}(t), \hat{V}(t)).$$

Proof. Part (i). Assume that $\mathcal{R}_i < 1$. Then Lemma 4 implies that $\rho(\Phi_{F^{(\cdot)}-\mathcal{V}^{(\cdot)}}(\tau)) < 1$. Thus, we can choose $j_0 > 0$ small enough such that $\rho(\Phi_{G_{j_0}(\cdot)}(\tau)) < 1$, where

$$G_{j_0}(t) = \begin{pmatrix} -\delta & [1-\Omega_I(t)]\left[\beta_l(T_l^*+j_0)+\beta_h(T_h^*+j_0)\right] \\ p & -[c+\Omega_c(t)] \end{pmatrix}.$$

From the first and the second equations of system (1), we have

$$\begin{cases} \frac{dT_l}{dt} \leq \lambda + qT_h - (d+r)T_l, \\ \frac{dT_h}{dt} \leq rT_l - (d+q)T_h. \end{cases} \tag{22}$$

By comparison principle, system (22), and Lemma 2, we see that

$$\limsup_{t\to\infty}(T_l(t), T_h(t)) \leq (T_l^*, T_h^*).$$

Therefore, there exists t_{j_0} such that $T_l(t) \leq T_l^* + j_0$, $T_h(t) \leq T_h^* + j_0$, $\forall t \geq t_{j_0}$. Then from the third and the fourth equations of system (1), we have

$$\begin{cases} \frac{dI}{dt} \leq -\delta I + [1-\Omega_I(t)]\left[\beta_l(T_l^*+j_0)+\beta_h(T_h^*+j_0)\right]V, \ t \geq t_{j_0}, \\ \frac{dV}{dt} = pI - [c+\Omega_c(t)]V, \ t \geq t_{j_0}. \end{cases} \tag{23}$$

Now, we consider the following auxiliary system

$$\begin{cases} \frac{dI}{dt} = -\delta I + [1-\Omega_I(t)]\left[\beta_l(T_l^*+j_0)+\beta_h(T_h^*+j_0)\right]V, \ t \geq 0, \\ \frac{dV}{dt} = pI - [c+\Omega_c(t)]V, \ t \geq 0. \end{cases} \tag{24}$$

According to Lemma 2.1 in [41], there exists a positive, τ-periodic function $(\bar{I}(t), \bar{V}(t))^T$ such that $e^{\Theta t}(\bar{I}(t), \bar{V}(t))^T$ is a solution of system (24), where $\Theta := \frac{1}{\tau}\ln(\rho(\Phi_{G_{j_0}(\cdot)}(\tau))) < 0$, due to the fact $\rho(\Phi_{G_{j_0}(\cdot)}(\tau)) < 1$. For any non-negative solution $(T_l(t), T_h(t), I(t), V(t))^T$ of system (1), we can choose a sufficiently large $m > 0$ satisfying $(I(t_{j_0}), V(t_{j_0}))^T \leq m(\bar{I}(t_{j_0}), \bar{V}(t_{j_0}))^T$. Clearly, $me^{\Theta(t-t_{j_0})}(\bar{I}(t), \bar{V}(t))^T$ is also a solution of (24), for all $t \geq t_{j_0}$. By the comparison principle (see [33,42]), we get

$$(I(t), V(t))^T \leq me^{\Theta(t-t_{j_0})}(\bar{I}(t), \bar{V}(t))^T, \ \forall t \geq t_{j_0}.$$

Since $\Theta < 0$, it follows that $(I(t), V(t))^T \to (0,0)^T$ as $t \to \infty$. Thus, (T_l, T_h) in system (1) is asymptotic to system (6). By the theory of asymptotically periodic semiflows (see, e.g., [43] or section 3.2 of [44]) and Lemma 2, it follows that $\lim_{t\to\infty}(T_l(t), T_h(t)) = (T_l^*, T_h^*)$. This completes the proof of Part (i).

Part (ii). We next consider the case where $\mathcal{R}_i > 1$. From Lemma 1, it follows that the discrete-time system $\{P^n\}_{n\geq 0}$ admits a global attractor in $\mathbb{X}$. Now we prove that $\{P^n\}_{n\geq 0}$ is uniformly persistent with respect to $(\mathbb{X}_0, \partial\mathbb{X}_0)$. By Lemma 5, it follows that $\mathbb{X}_0$ and $\partial\mathbb{X}_0$ are positively invariant under the solution flow of (1). Clearly, $\mathbb{X}_0 \cup \partial\mathbb{X}_0 = \mathbb{X}$, $\mathbb{X}_0 \cap \partial\mathbb{X}_0 = \emptyset$, and $\partial\mathbb{X}_0$ is relatively closed in $\mathbb{X}$.

Let

$$M_\partial = \{(T_{l0}, T_{h0}, I_0, V_0) \in \partial\mathbb{X}_0 : P^n(T_{l0}, T_{h0}, I_0, V_0) \in \partial\mathbb{X}_0, \ \forall\, n \geq 0\}.$$

Next, we show that

$$M_\partial := \{(T_{l0}, T_{h0}, I_0, V_0) \in \mathbb{X} :, I_0 = V_0 = 0\}. \tag{25}$$

For the establishment of (25), we note that it suffices to prove that for any $(T_{l0}, T_{h0}, I_0, V_0) \in M_\partial$ and for any $m \geq 0$, we have $I(m\tau) = V(m\tau) = 0$. If it is not true, then there exists $m_1 \geq 0$ such that $(T_{l0}, T_{h0}, I_0, V_0) \in M_\partial$ with

$$(I(m_1\tau), V(m_1\tau)) \neq (0,0).$$

Then the irreducibility of the cooperative matrix (17) implies that

$$(I(m\tau), V(m\tau))^T \gg (0,0), \ \forall\, m > m_1.$$

This contradicts the definition of M_∂, and hence, (25) is true.

Obviously, there is a unique fixed point of P in M_∂, which is $E_0 = (T_l^*, T_h^*, 0, 0)$. If $(T_l(t), T_h(t), I(t), V(t))$ is a nonnegative solution of system (1) initiating from M_∂, it is not hard to see that $(T_l(t), T_h(t), I(t), V(t))$ approaches E_0 as t approaches ∞, that is, every orbit of P in M_∂ approaches to $\{E_0\}$.

In view of Lemma 6, we see that $\{E_0\}$ is an isolated invariant set in $\mathbb{X}$ and $W^s(E_0) \cap \mathbb{X}_0 = \emptyset$, where $W^s(E_0)$ is the stable set of E_0, and $\{E_0\}$ is acyclic in M_∂. By Theorem 1.3.1 in [44], it follows that $\{P^n\}_{n\geq 0}$ is uniformly persistent with respect to $(\mathbb{X}_0, \partial\mathbb{X}_0)$. By Theorem 3.1.1 in [44], the solutions of system (1) are uniformly persistent with respect to $(\mathbb{X}_0, \partial\mathbb{X}_0)$, that is, there exists an $\zeta > 0$ such that for any solution $(T_l(t), T_h(t), I(t), V(t))$ with initial value $(T_{l0}, T_{h0}, I_0, V_0) \in \mathbb{X}_0$ satisfies

$$\liminf_{t\to\infty} I(t) \geq \zeta, \ \liminf_{t\to\infty} V(t) \geq \zeta.$$

Furthermore, Theorem 1.3.6 in [44] implies that P has a fixed point

$$(\hat{T}_l(0), \hat{T}_h(0), \hat{I}(0), \hat{V}(0)) \in \mathbb{X}_0,$$

and hence, $\hat{I}(0) > 0$, $\hat{V}(0) > 0$. Thus, $(\hat{T}_l(t), \hat{T}_h(t), \hat{I}(t), \hat{V}(t))$ is a τ-periodic solution of system (1) with $\hat{I}(0) > 0$, $\hat{V}(0) > 0$. By the similar arguments to those in Lemma 5, we can further show that

$$(\hat{T}_l(t), \hat{T}_h(t), \hat{I}(t), \hat{V}(t)) \gg 0.$$

This completes the proof of Part (ii). □

4. Numerical computation: role of morphine pharmacodynamics and periodic intake

In this section, we present results from the numerical computations performed to study the role of morphine pharmacodynamics in different aspects of viral dynamics within drug abusers. Particularly, we focus on how parameters related to morphine pharmacodynamics affect the infection threshold ($\mathcal{R}_i$), viral load (vRNA copies per ml of plasma), and CD4 count (the total number of CD4+ T-cells per microliter of plasma). We use the results from Lemma 3, which states that the infection threshold ($\mathcal{R}_i$) can be obtained by solving $\rho(W(\tau,\theta)) = 1$ for θ to compute $\mathcal{R}_i$, and we obtain θ solution from $\rho(W(\tau,\theta)) = 1$ numerically. Furthermore, we solve the model system (1) numerically in MATLAB to evaluate the influence of the pharmacodynamic parameters on the viral load and CD4 count.

We obtain some of the model parameters from previously published literature and the remaining parameters are estimated and/or assumed. Specifically, we refer studies on basic viral dynamics [45–47] and morphine conditioning viral dynamics [13,48] for base-case parameters used in our simulations. All model parameters along with description, their values, and sources are provided in Table 1. Viral dynamics for the first 200 days predicted by the model with the base-case parameters (Table 1), which gives $\mathcal{R}_i \sim 4.5$ (IVM) and ~ 5.9 (SROM), are shown in Fig. 3. Clearly, the infection persists as $\mathcal{R}_i > 1$, consistent with our theoretical result. However, the parameters used here did not correspond to the periodic solution with a large amplitude. We also perform a sensitivity analysis of those parameters which were not available and assumed. Sensitivity of peak viral load and set point viral load on hundreds of parameter sets selected randomly from a wide range of uncertain parameters (η, σ, M_h, n) indicates that the model is robust across these uncertain parameters within a reasonable range (Fig. 3). We now discuss the results for two routes of morphine intake, IVM and SROM, separately.

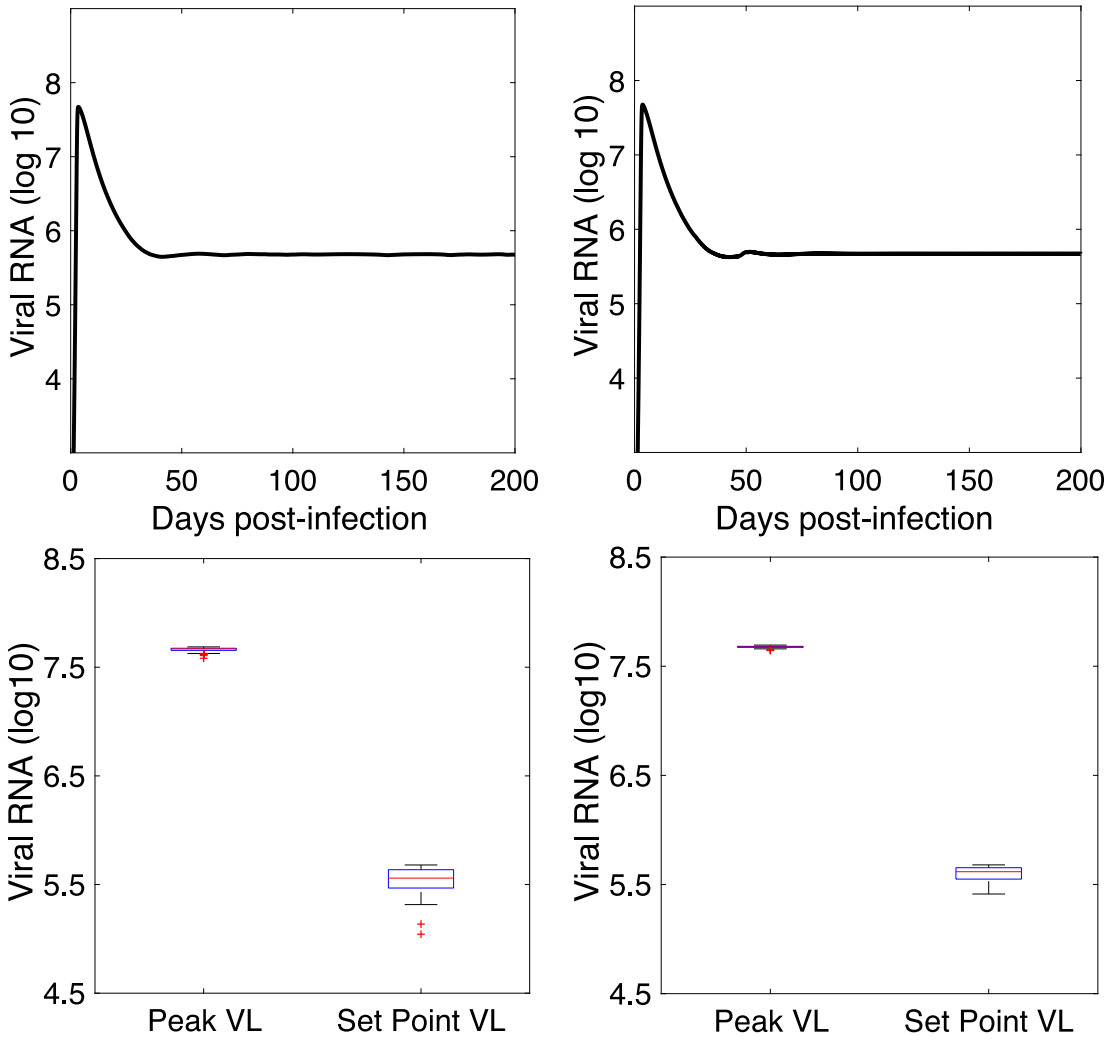

Fig. 3. Model prediction of viral dynamics for the first 200 days post infection (first row) and sensitivity of peak viral load and set point viral load (second row) for IVM case (first column) and SROM case (second column).

Table 1
Model parameters.

Description	Parameter	Estimate	Source
Reproduction rate of T cells	λ	3630 cells ml^{-1} day^{-1}	[13,48]
Infection rate of T_l	β_l	2.29×10^{-9} day^{-1}	Estimate, [13,48]
Infection rate of T_h	β_h	2.29×10^{-7} day^{-1}	Estimate, [13,48]
Death rate of uninfected T cells	d	0.01 day^{-1}	[45,47]
Death rate of infected T cells	δ	0.65 day^{-1}	Estimate, [48]
Virion production rate	p	2500 day^{-1}	[48]
Virion clearance rate	c	23 day^{-1}	[46]
Transition rate from T_l to T_h	r	0.15 day^{-1}	[48]
Transition rate from T_h to T_l	q	0.18 day^{-1}	[48]
Net $A(t)$ effect scaling factor	η	0.8 ml ng^{-1}	Assumed
Net $A(t)$ effect scaling factor	σ	0.5 day^{-1}	Assumed
Time morphine concentration is half	M_h	50 days	Assumed
Hill's coefficient	n	5	Assumed
Morphine dose	a_0	100 [0–200]	Varied
Morphine half life	$t_{1/2}$	4 [1–10] hours	Varied
Morphine mean level	M_0	100 [50–200]	Varied
Amplitude	a	50 [0–100]	Varied
Drug intake interval	τ	8 [2–22] hours	Varied

4.1. Intravenous morphine (IVM)

In this case, morphine pharmacodynamics parameters are morphine dose, a_0, morphine half-life, $t_{1/2} = \ln(2)/b_1$, and drug interval, τ. With all other parameters fixed as the values in Table 1, we vary a_0, $t_{1/2}$, and τ to observe their effects on $\mathcal{R}_i$, viral load, and CD4 count.

Infection threshold, $\mathcal{R}_i$. As shown in Fig. 4, each of the morphine pharmacodynamics parameters can affect the value of $\mathcal{R}_i$. In general, an increase in morphine dose and/or a half-life increases $\mathcal{R}_i$, while an increase in drug interval decreases $\mathcal{R}_i$ (Fig. 4). In particular, a morphine dose greater than 50 (i.e., $a_0 > 50$) causes a faster increase in $\mathcal{R}_i$ (Fig. 4(a)), resulting in the value of $\mathcal{R}_i$ about 6 for $a_0 = 200$, which is

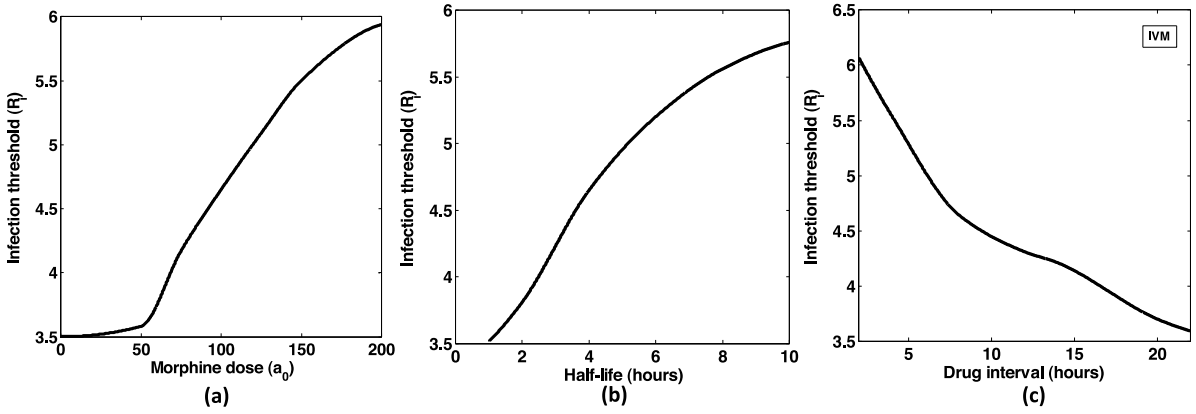

Fig. 4. Viral infection threshold, $\mathcal{R}_i$, as a function of (a) the morphine dose, a_0, (b) the half-life of morphine, $t_{1/2}$, and (c) the morphine intake interval, τ, in IVM route.

quite high compared to the value of $\mathcal{R}_i = 3.5$ in the absence of morphine ($a_0 = 0$). Similarly, an increase in half-life from 1 hr to 10 hr can cause to increase $\mathcal{R}_i$ from 3.5 to 5.7 (Fig. 4(b)). Also, a higher frequency of morphine intake, such as intake of every 2 hr instead of every 22 hr, can drastically raise the value of $\mathcal{R}_i$ ($\mathcal{R}_i = 6.1$ for $\tau = 2$ hr and $\mathcal{R}_i = 3.6$ for $\tau = 22$ hr) (Fig. 4(c)). Since our parameters correspond to infected hosts, the value of $\mathcal{R}_i$ is greater than 1 for all the range of morphine pharmacodynamics as expected, showing that the morphine pharmacodynamics do not play a role in determining whether infection occurs or is avoided. However, the effects of morphine pharmacodynamics on $\mathcal{R}_i$ obtained here can be critical in the case when antiretroviral therapy, including pre-exposure prophylaxis, is used.

Viral load and CD4 count. For the purpose of demonstration, we use our model to compute viral load and CD4 count at the end of 200 days post infection. Our results (Fig. 5(a)) show that an increase in the morphine dose from $a_0 = 0$ to $a_0 = 200$ increases the viral load at the end of 200 days post infection from 5.59 $\log_{10}$ to 5.67 $\log_{10}$. In this case the day 200 post infection CD4 count decreases from 354 to 256 (Fig. 5(c)). Similarly, increasing the morphine half-life from 1 to 10 h increases the day 200 post infection viral load from 5.58 $\log_{10}$ to 5.67 $\log_{10}$ (Fig. 5(b)) and decreases the CD4 count from 353 to 260 (Fig. 5(d)). Therefore, the morphine pharmacodynamics related to IVM route can have noticeable effects on both viral load and CD4 count in HIV-infected drug abusers.

4.2. Slow-release oral morphine (SROM)

As discussed earlier the profile of morphine through SROM route can be described with sinusoidal function with three main parameters: M_0 (the mean level of morphine), a (morphine amplitude), and τ (morphine intake interval). Here, we use our model to compute $\mathcal{R}_i$, viral load and CD4 count for different values of M_0, a, and τ, while all other parameters are fixed at the values in Table 1.

Infection threshold, $\mathcal{R}_i$. As in IVM case, here also, the value of $\mathcal{R}_i$ remains greater than 1 for all range of parameters considered as expected because of our base parameter values that correspond to infected host. As shown in Fig. 6(a), an increase in the mean level of morphine increases $\mathcal{R}_i$ with a pronounced increase for the mean level between 50 and 125 (i.e., $4.8 \leq \mathcal{R}_i \leq 6.3$ for $50 \leq M_0 \leq 125$). This effect on $\mathcal{R}_i$ from increasing M_0 eventually saturates with almost no change in $\mathcal{R}_i$ for $M_0 > 125$ (Fig. 6(a)). Similarly, an increase in amplitude diseases $\mathcal{R}_i$ with a larger decrease in $\mathcal{R}_i$ when the amplitude increases from 25 to 100 (Fig. 6(b)). Furthermore, our results show that increasing interval for morphine intake from 2 hours to 8 hours slightly decreases $\mathcal{R}_i$ from 6.2 to 5.9 (Fig. 6(c)), but $\mathcal{R}_i$ remains almost constant for morphine intake interval greater than 8 hours.

Viral load and CD4 count. Again, we compute viral load and CD4 count at the end of 200 days post infection for varying morphine pharmacodynamics parameters related to SROM route. An increase in the mean level of morphine increases the day 200 post infection viral load from 5.14 $\log_{10}$ to 5.27 $\log_{10}$ whereas an increase in the amplitude decreases the viral load from 5.26 $\log_{10}$ to 5.01 $\log_{10}$ (Fig. 7(a) and 7(b)). These results suggest that the morphine pharmacodynamics play a minimal role in altering the viral load in the morphine intake route SROM compared to the IVM route. However, we found comparable effects on CD4 count in both SROM and IVM routes. For example, an increase in the mean level of morphine dose from 0 to 200 decreases the CD4 count from 340 to 246 (Fig. 7(c)), and an increase in the amplitude from 0 to 10 increases the CD4 count from 250 to 287 (Fig. 7(d)).

5. Conclusion

In this study, we developed a mathematical model to describe HIV virus and antibody dynamics under morphine (drugs of abuse) conditioning with periodic intake. We considered pharmacodynamics of morphine administered through two commonly practiced routes: (i) intravenous morphine (IVM), in which morphine is directly administered into the circulation providing a rapid effect [20], and (ii) slow release oral morphine (SROM), in which morphine is slowly released into the circulation during pharmacotherapy maintenance treatment for opioid-dependent individuals [23–30]. Our model is capable of capturing the time-dependent nature of morphine concentration within a host, allowing us to properly study the effects of morphine pharmacodynamics as well as the frequency of morphine intake, which are important factors for virus dynamics in drug abusers. Moreover, two entirely different time-dependent patterns embedded in the model resulting from two routes of morphine intake have provided further insights into the role of immune response in virus control under conditioning of drugs of abuse.

We successfully analyzed our non-autonomous model, establishing stability theorems for global dynamics of the system. The rigorous mathematical techniques implemented for our model can also be used in other non-autonomous systems of infection dynamics, for which analytical methods are still limited. In particular, we formulated the infection threshold, $\mathcal{R}_i$, that completely determines the viral dynamics under periodic morphine intake and provides a condition for infection to persist ($\mathcal{R}_i > 1$) or die out ($\mathcal{R}_i < 1$). Importantly, $\mathcal{R}_i$ highly depends on parameters related to morphine pharmacodynamics and periodic intake in both IVM and SROM routes. In addition, we also performed numerical computations of our model to demonstrate that morphine pharmacodynamics can have significant impact on viral load and CD4 counts in HIV-infected drug abusers.

We acknowledge some limitations of our study. Our simulation results are based on parameters estimated from limited data sets. More realistic parameters, including those related to morphine and antibody responses, may help improve our results. We introduced explicit relationship between antibody response and morphine concentration.

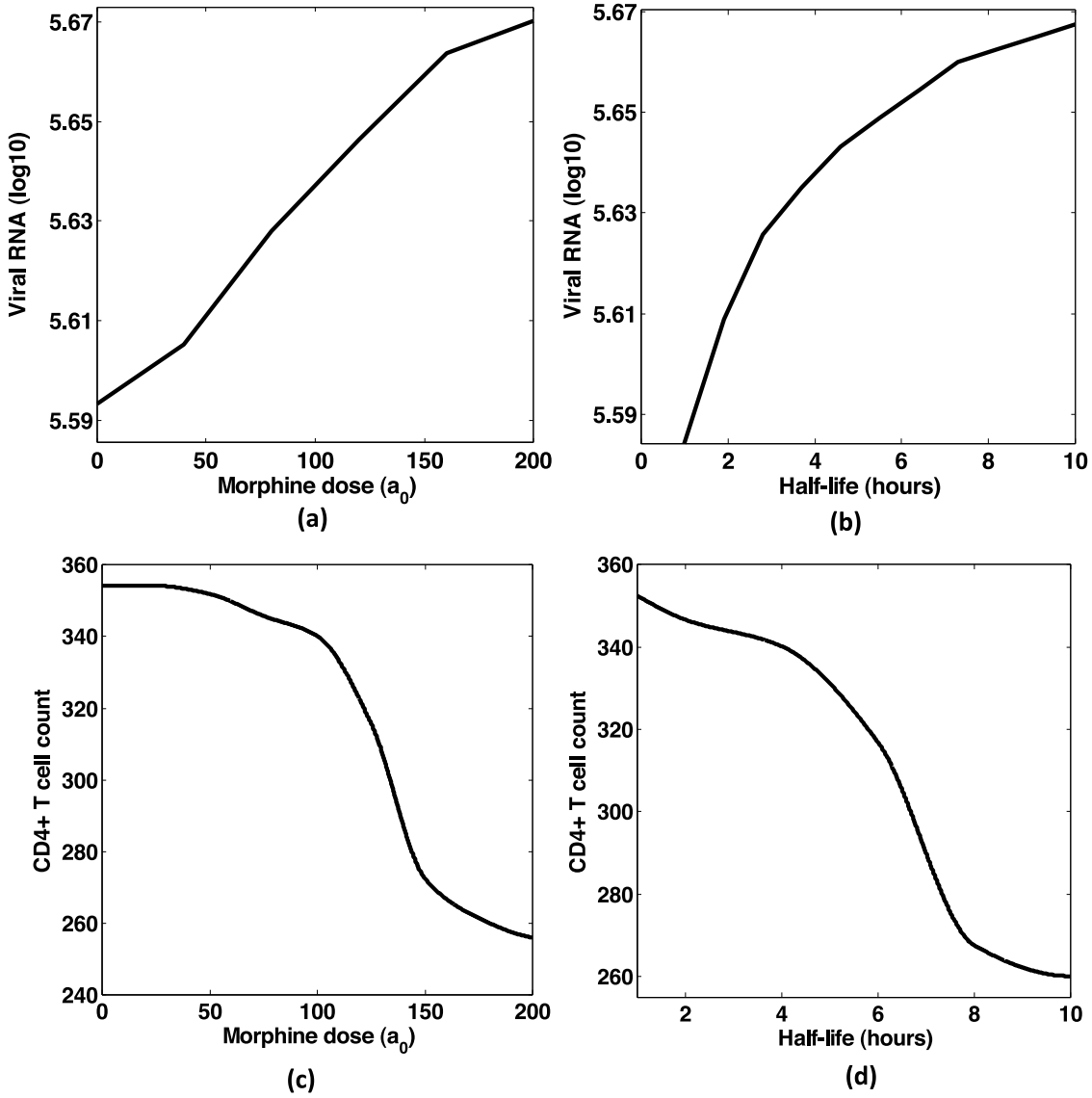

Fig. 5. Changes in viral load and CD4 count with varying morphine dose, a_0, and morphine half-life, $t_{1/2}$, in IVM route.

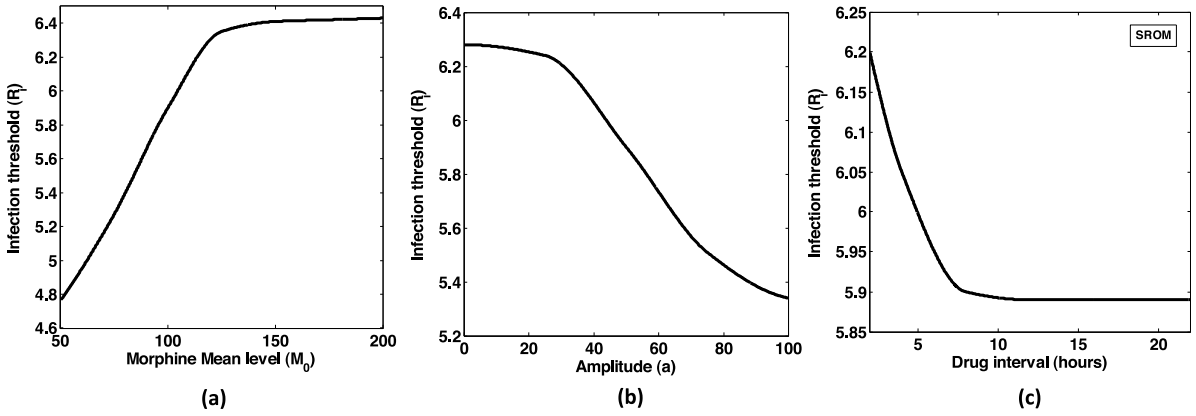

Fig. 6. Viral infection threshold, $\mathcal{R}_i$, as a function of (a) the mean level of morphine, M_0, (b) the morphine amplitude, a, and (c) the morphine intake interval, τ, in SROM route.

Also, we included the effects of virus particles on antibody production implicitly via the time-dependent functional form of antibody. While this approach was validated by the experimental data in previous studies [13,19], modeling a detailed role of virus particles in antibody production may be beneficial for accurate evaluations of morphine intake. However, such complicated models may require rich data sets

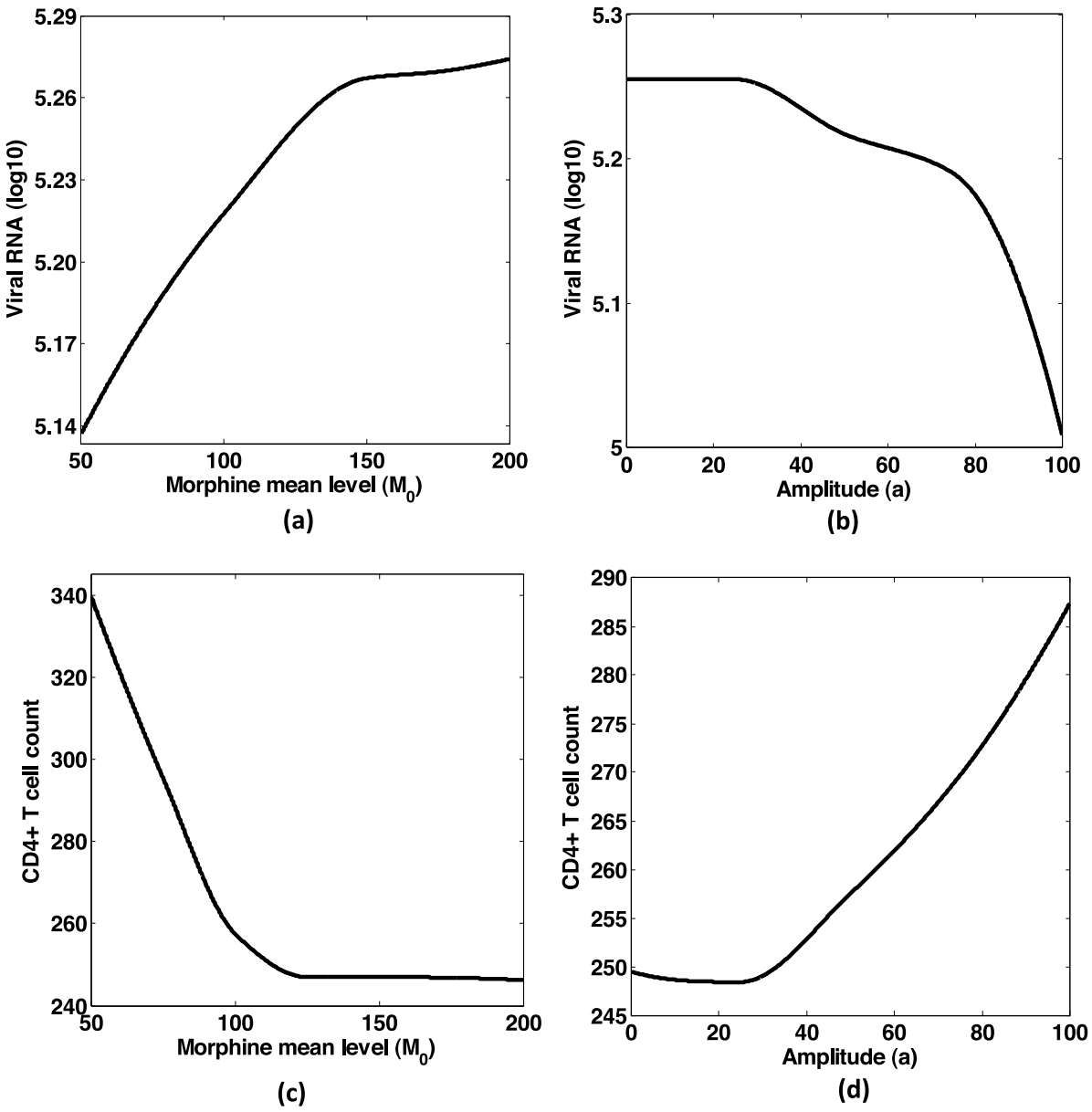

Fig. 7. Changes in viral load and CD4 count with varying mean level of morphine, M_0, and the morphine amplitude, a, in SROM route.

related to mechanisms of altering antibody levels due to virus in the presence of morphine. For the IVM case, we did not consider the residual morphine from the previous period at the beginning of the next period. While this assumption is valid for our base-case computations, a detailed modeling of residual morphine results in an impulsive system. The mathematical formulation of the reproduction ratio for such impulsive differential equation systems as in Bai and Zhao [49] may be quite different from the periodic system considered in this study. Because of complexity of the model, we are unable to find the closed form of infected equilibrium and unable to establish its uniqueness. Instead we have established its existence only.

In summary, our study provides a model and techniques for evaluating periodic intake of drugs of abuse on HIV infection dynamics within a host. Our analytical and simulation results offer several interesting findings that can be beneficial to develop proper guidelines for successful HIV control and prevention strategies, including development of antibody-based vaccines and pre-exposure prophylaxis, for drug abusers.

Declaration of competing interest

The authors declare that they have no known competing financial interests or personal relationships that could have appeared to influence the work reported in this paper.

Acknowledgments

This work was funded by NSF grants DMS-1616299 (NKV) and DMS-1836647 (NKV) from National Science Foundation, United States, and UGP award (NKV) and the start-up fund (NKV) from San Diego State University. Research of FBW is supported in part by Ministry of Science and Technology, Taiwan; and National Center for Theoretical Sciences, National Taiwan University; and Chang Gung Memorial Hospital, Taiwan (CRRPD3H0011, BMRPD18, NMRPD5J0201 and CLRPG2H0041). NKV would like to thank National Center for Theoretical Sciences, National Taiwan University for providing support for NCTS visit, during which some of the work was carried out.

References

[1] UNAIDS, The joint united nations programme on HIV and AIDS (UNAIDS), in: Global Report, 2013, Retrieved on October 10, 2017. http://files.unaids.org/en/media/unaids/contentassets/documents/epidemiology/2013/gr2013/UNAIDS_Global_Report_2013_en.pdf.

[2] UNAIDS, The joint united nations programme on HIV and aids, fact sheet 2017 global HIV statistics, 2017, Retrieved on January 20, 2018. http://www.unaids.org/sites/default/files/media_asset/UNAIDS_FactSheet_en.pdf.

[3] R.M. Donahoe, D. Vlahov, Opiates as potential cofactors in progression of HIV-1 infections to AID, J. Neuroimmunol. 83 (1998) 77–87.

[4] P.V.B. Reddy, S. Pilakka-Kanthikeel, S.K. Saxena, Z. Saiyed, M.P.N. Nair, Interactive effects of morphine on HIV infection: Role in HIV-associated neurocognitive disorder, Aids Res. Treat. 2012 (2012) http://dx.doi.org/10.1155/2012/953678.

[5] Center for Disease Control (CDC), Epidemiology of HIV infection through 2012, 2012, Retrieved on October 10, 2017. https://www.cdc.gov/hiv/pdf/statistics_surveillance_epi-hiv-infection.pdf.

[6] H. Friedman, C. Newton, T.W. Klein, Microbial infections, immunomodulation, and drugs of abuse, Clin. Microbiol. Rev. 16 (2003) 209–219.

[7] R. Kumar, C. Torres, T. Yamamura, I. Rodriguez, S.S. Martinez, R.M. Donahoe, E. Kraiselburd, E.B. Stephens, A. Kumar, Modulation by morphine of viral point in rhesus macaques infected with simian immunodeficiency virus and simian-human immunodeficiency virus, J. Virol. 78 (20) (2004) 11425–11428.

[8] R. Kumar, S. Orsoni, L. Norman, A.S. Verma, G. Tirado, L.D. Giavedoni, S. Staprans, G.M. Miller, S.J. Buch, A. Kumar, Chronic morphine exposure causes pronounced virus replication in cerebral compartment and accelerated onset of AIDS in SIV/SHIV-infected Indian rhesus macaques, Virology 354 (2006) 192–206.

[9] P.J. Ronald, J.R. Robertson, R.A. Elton, Continued drug use and other cofactors for progression to AIDS among injecting drug users, AIDS 8 (3) (1994) 339–343.

[10] Y. Wang, X. Wang, L. Ye, J. Li, L. Song, N. Fulambarkar, W. Ho, Morphine suppresses IFN signaling pathway and enhances AIDS virus infection, Plos ONE 7 (2) (2012) http://dx.doi.org/10.1371/journal.pone.0031167, e31167.

[11] J. Overbaugh, L. Morris, The antibody response against HIV-1, Cold Spring Harb Perspect Med. (2012) 2012;2:a007039.

[12] S. Bonhoeffer, R.M. May, G.M. Shaw, M.A. Nowak, Virus dynamics and drug therapy, Proc. Natl. Acad. Sci. USA 94 (13) (1997) 6971–6976.

[13] J.M. Mutua, A.S. Perelson, A. Kumar, N.K. Vaidya, Modeling the effects of morphine-altered virus specific antibody responses on HIV/siv dynamics, Sci. Rep. 9 (1) (2019) 5423, http://dx.doi.org/10.1038/s41598-019-41751-8.

[14] M.A. Nowak, R.M. May, Virus Dynamics: Mathematical Principles of Immunology and Virology, Oxford University Press, New York, 2000.

[15] A.S. Perelson, Modelling viral and immune system dynamics, Nat. Rev. Immunol. 2 (1) (2012) 28–36.

[16] A.S. Perelson, R.M. Ribeiro, Modeling the within-host dynamics of HIV infection, BMC Biol. 11 (96) (2013) 1–10.

[17] N.K. Vaidya, L. Rong, Modeling pharmacodynamics on HIV latent infection: Choice of drugs is key to successful cure via early therapy, SIAM J. Appl. Math 77 (5) (2017) 1781–1804.

[18] Y. Chao, W. Wang, Modeling HIV dynamics under combination therapy with inducers and antibodies, Bull. Math. Biol. 81 (2019) 2625–2648, http://dx.doi.org/10.1007/s11538-019-00621-0.

[19] G.D. Tomaras, N.L. Yates, P. Liu, L. Qin, G.G. Fouda, L.L. Chavez, et al., Initial B-cell responses to transmitted human immunodeficiency virus type 1: Virion-binding immunoglobulin M (IgM) and IgG antibodies followed by plasma anti-gp41 antibodies with ineffective control of initial viremia, J. Virol. 82 (2008) 12449–12463.

[20] S. Mercadante, Intravenous morphine for management of cancer pain, Lancet Oncol. 11 (5) (2010) 484–489.

[21] J. Lötsch, Pharmacokinetic-pharmacodynamic modeling of opioids, J. Pain Symptom Manag. 29 (5 Suppl) (2005) 90–103.

[22] K.T. Olkkola, E. Maunuksela, R. Korpela, P.H. Rosenberg, Kinetics and dynamics of postoperative intravenous morphine in children, Clin. Pherm. Therap. 44 (2) (1987) 128–136.

[23] M. Ferri, S. Minozzi, A. Bo, L. Amato, Slow-release oral morphine as maintenance therapy for opioid dependence, Cochrane Database Syst. Rev. (6) (2013) CD009879, http://dx.doi.org/10.1002/14651858.CD009879.pub2.

[24] T. Beck, C. Haasen, U. Verthein, S. Walcher, C. Schuler, M. Backmund, C. Ruckes, J. Reimer, Maintenance treatment for opioid dependence with slow-release oral morphine: A randomized cross-over, non-inferiority study versus methadone, Addiction 109 (2013) 617–626.

[25] H. Eder, R. Jagsch, D. Kraigher, A. Primorac, N. Ebner, G. Fischer, Comparative study of the effectiveness of slow release morphine and methadone for opioid maintenance therapy, Addiction 100 (2005) 1101–1109.

[26] G. Fischer, O. Presslich, K. Diamant, C. Schneider, L. Pezawas, S. Kasper, Oral morphine-sulphate in the treatment of opiate dependent patients, Alcoholism 32 (1996) 35–43.

[27] P. Hermann, W. Wagner, B. Lindenbauer, Safety and efficacy of oral prolonged release morphine for the maintenance therapy for opioid dependence - Results of a pilot study in outpatients, SFP 7 (2005) 215–220.

[28] D. Kraigher, R. Jagsch, W. Gombas, R. Ortner, H. Eder, A. Primorac, et al., Use of slow-release oral morphine for the treatment of opioid dependence, Eur Addict Res. 11 (2005) 145–151.

[29] T.B. Mitchell, J.M. White A.A. Somogyi, F. Bochner, Slow release morphine versus methadone: A crossover comparison of patient outcomes and acceptability as maintenance pharmacotherapies for opioid dependence, Addiction 99 (2004) 940–945.

[30] G.N. Vasilev, D.Z. Alexieva, R.Z. Pavlova, Safety and efficacy of oral slow release morphine for maintenance treatment in heroin addicts: A 6-month open non comparative study, Eur. Addict. Res. 12 (2006) 53–60.

[31] M.E. Socías, E. Wood, Evaluating slow-release oral morphine to narrow the treatment gap for opioid use disorders, Ann. Intern Med. 168 (2) (2018) 141–142.

[32] T.B. Mitchell, J.M. White, A.A. Somogyi, F. Bochner, Comparative pharmacodynamics and pharmacokinetics of methadone and slow-release oral morphine for maintenance treatment of opioid dependence, Drug Alcohol Depend. 72 (2003) 85–94.

[33] H.L. Smith, Monotone dynamical systems: An introduction to the theory of competitive and cooperative systems, Math. Surv. Monogr. 41 (1995).

[34] J. Hale, Asymptotic Behavior of Dissipative Systems, American Mathematical Society Providence, RI, 1988.

[35] N. Bacaër, S. Guernaoui, The epidemic threshold of vector-borne diseases with seasonality. The case of cutaneous leishmaniasis in Chichaoua, Morocco, J. Math. Biol. 53 (2006) 421–436.

[36] W. Wang, X.Q. Zhao, Threshold dynamics for compartmental epidemic models in periodic environments, J. Dyn. Diff. Equat. 20 (3) (2008) 699–717.

[37] J. Jiang, On the global stability of cooperative systems, Bull. Lond. Math. Soc. 26 (1994) 455–458.

[38] N.K. Vaidya, L.M. Wahl, Avian influenza dynamics under periodic environmental conditions, SIAM J. Appl. Math. 75 (2) (2015) 443–467.

[39] L. Liu, X.Q. Zhao, Y. Zhou, A tuberculousis model with seasonality, Bull. Math. Biol. 72 (2010) 931–952.

[40] P.V.d. Driessche, J. Watmough, Reproduction numbers and sub-threshold endemic equilibria for compartmental models of disease transmission, Math. Biosci. 180 (2002) 29–48.

[41] F. Zhang, X.Q. Zhao, A periodic epidemic model in a patchy environment, J. Math. Anal. Appl. 325 (2007) 496–516.

[42] H.L. Smith, P. Walman, The Theory of the Chemostat, Cambridge University Press, Cambridge, 1995.

[43] X.Q. Zhao, Asymptotic behavior for asymptotically periodic semiflows with applications, Commun. Appl. Nonlinear Anal. 3 (1996) 43–66.

[44] X.Q. Zhao, Dynamical Systems in Population Biology, Springer, New York, 2003.

[45] H. Mohri, S. Bonhoeffer, S. Monard, A.S. Perelson, D.D. Ho, Rapid turnover of T lymphocytes in SIV-infected rhesus macaques, Science 279 (5354) (1998) 1223–1227.

[46] B. Ramratnam, S. Bonhoeffer, J. Binley, A. Hurley, L. Zhang, J. Mittler, M. Markowitz, J.P. Moore, A.S. Perelson, D.D. Ho, Rapid production and clearance of HIV-1 and hepatitis C virus assessed by large volume plasma apheresis, Lancet 354 (9192) (1999) 1782–1785.

[47] M.A. Stafford, L. Corey, Y. Cao, E.S. Daar, D.D. Ho, A.S. Perelson, Modeling plasma virus concentration during primary HIV infection, J. Theoret. Biol. 203 (3) (2000) 285–301.

[48] N.K. Vaidya, R.M. Ribeiro, A.S. Perelson, A. Kumar, Modeling the effects of morphine on simian immunodeficiency virus dynamics, PLoS Comput. Biol. 12 (9) (2016) e1005127, http://dx.doi.org/10.1371/journal.pcbi.1005127.

[49] Z. Bai, X.-Q. Zhao, Basic reproduction ratios for periodic and time-delayed compartmental models with impulses, Math. Biol. 80 (2020) 1095–1117.